ASME Journal of Biomechanical Engineering
Online journal at:
https://asmedigitalcollection.asme.org/biomechanical

Kyle D. Meadows
Biomedical Engineering,
University of Delaware,
Newark, DE 19716

John M. Peloquin
Biomedical Engineering,
University of Delaware,
Newark, DE 19716

Milad I. Markhali
Biomedical Engineering,
University of Delaware,
Newark, DE 19716

Miltiadis H. Zgonis
Department of Orthopaedic Surgery,
Penn Medicine,
University of Pennsylvania,
Philadelphia, PA 19104

Thomas P. Schaer
Department of Clinical Studies,
New Bolton Center,
School of Veterinary Medicine,
University of Pennsylvania,
Philadelphia, PA 19104

Robert L. Mauck
McKay Orthopaedic Research Laboratory,
University of Pennsylvania,
Philadelphia, PA 19104;
Translational Musculoskeletal Research Center,
CMC VA Medical Center,
Philadelphia, PA 19104

Dawn M. Elliott[1]
Biomedical Engineering,
University of Delaware,
201 STAR Health Sciences Center,
Newark, DE 19716
e-mail: delliott@udel.edu

Acute Repair of Meniscus Root Tear Partially Restores Joint Displacements as Measured With Magnetic Resonance Images and Loading in a Cadaveric Porcine Knee

The meniscus serves important load-bearing functions and protects the underlying articular cartilage. Unfortunately, meniscus tears are common and impair the ability of the meniscus to distribute loads, increasing the risk of developing osteoarthritis. Therefore, surgical repair of the meniscus is a frequently performed procedure; however, repair does not always prevent osteoarthritis. This is hypothesized to be due to altered joint loading post-injury and repair, where the functional deficit of the meniscus prevents it from performing its role of distributing forces. The objective of this study was to quantify joint kinematics in an intact joint, after a meniscus root tear, and after suture repair in cadaveric porcine knees, a frequently used in vivo model. We utilized an magnetic resonance images-compatible loading device and novel use of a T_1 vibe sequence to measure meniscus and femur displacements under physiological axial loads. We found that anterior root tear led to large meniscus displacements under physiological axial loading and that suture anchor repair reduced these displacements but did not fully restore intact joint kinematics. After tear and repair, the anterior region of the meniscus moved posteriorly and medially as it was forced out of the joint space under loading, while the posterior region had small displacements as the posterior attachment acted as a hinge about which the meniscus pivoted in the axial plane. Methods from this study can be applied to assess altered joint kinematics following human knee injuries and evaluate repair strategies aimed to restore joint kinematics.
[DOI: 10.1115/1.4062524]

Keywords: MRI, meniscus, tear, repair, kinematics

Introduction

The meniscus serves important load-bearing functions at the knee and protects the underlying articular cartilage. Unfortunately, meniscus tears are a common condition that impairs the ability of the meniscus to distribute loads and, without surgical treatment, greatly increases the risk of developing osteoarthritis (OA) [1–9]. Surgical meniscus repair is chondro-protective and can delay OA but does not halt degeneration for many patients [10,11]. It is often hypothesized that this is due to altered joint loading post-injury and repair, where the functional deficit of the meniscus prevents it from performing its role of distributing forces in the knee. Previous work has shown that there is a relationship between greater meniscal extrusion and joint degeneration [12–16]. Some studies have shown, using pressure sensors (e.g., TEK-SCAN) inserted into the joint space, that meniscus injury leads to larger peak forces and smaller contact areas on the tibial plateau; however, these studies required transecting the joint capsule and sometimes the lateral or medial collateral ligaments to make the measurement [2–4,17,18]. Therefore, as described below, noninvasive measurement of joint and meniscus kinematics is critical to understanding the impact of meniscus injury and repair on joint loading and chondroprotection.

Magnetic resonance images (MRI) acquired under different loading conditions allows for noninvasive measurement of joint kinematics without disrupting any joint tissues. While forces cannot be measured via MRI, kinematics, including displacements and

[1]Corresponding author.

Manuscript received December 5, 2022; final manuscript received May 2, 2023; published online May 31, 2023. Assoc. Editor: Joao S. Soares.

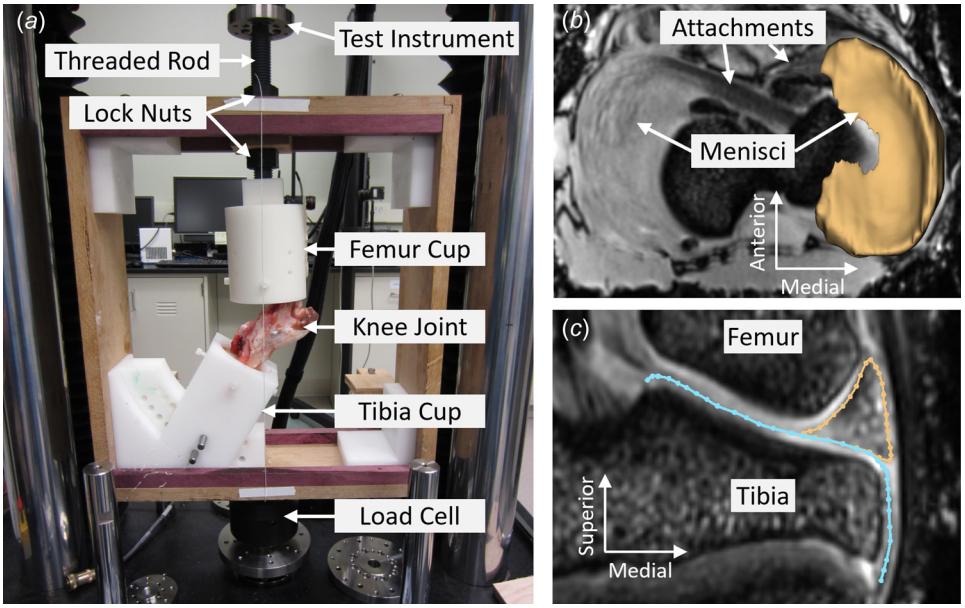

Fig. 1 (*a*) MRI compatible loading frame in the mechanical testing instrument (TA Electro-Force 3510). T1 vibe MRI of knee in (*b*) axial plane with 3D segmentation of medial meniscus overlayed, and (*c*) midcoronal plane with outlines of meniscus (gold) and tibial plateau (blue) overlayed. (Color version online.)

rotations of the meniscus and femur, can be measured in the intact joint. This is important as the collateral ligaments and joint capsule contribute meaningfully to joint kinematics. Two studies have utilized MRI to measure meniscus protrusion/extrusion at various flexion angles in healthy, uninjured subjects or in patients with OA, but not following a diagnosed meniscus injury [19,20]. Other work used MRI to measure three-dimensional (3D) strains in the meniscus at various degeneration levels, but either did not report femur or meniscus displacements or only studied healthy joints [21–23]. Additional work has measured cartilage deformations under loading using MRI-compatible loading devices or exercise, but meniscus findings were not reported [24–26]. Evaluation of meniscus repair methods would benefit from measurement of joint kinematics after surgery in an intact joint. Likewise, the application of novel imaging protocols, for example, T_1 vibe MRI for tracking meniscus and femur motion, allows for better imaging of the menisci than traditional clinical MRI used in other studies and would improve our understanding of meniscus function under load. Thus, the objective of this work was to measure changes in meniscus and femur displacements in an intact joint, following a meniscus root tear, and following suture repair at an acute time point using novel MRI methods to measure kinematics with the joint under axial load in porcine cadaver model. This in vitro work used a Yucatan minipig stifle joint, similar to our and other established animal model [3,4,27]. These models are clinically relevant due to their similarity to human joint size, load bearing, and immune systems [28–30]. Importantly, future studies can apply these methods to the human knee. We hypothesized that a root tear would cause meniscus extrusion and medial displacements of the femur and that a suture anchor repair would restore the meniscus to its near-intact position and kinematics.

Methods

To measure the effect of injury and repair on meniscus and femur displacements with loading, each joint was loaded and imaged in three experimental states: intact, tear, and repair.

Sample Preparation. Seven fresh-frozen Yucatan minipig hindlimbs, harvested from 12–18 month-old castrated males, were obtained (Sierra Medical for Sciences, Whittier, CA[2]). We chose this age range because the animals are skeletally mature and it matches the age of pigs that we have previously used in our live animal model [3,4]. After thawing for two days at 4 °C, all skin and musculature were removed from the stifle joint, with special care taken to preserve the joint capsule, lateral collateral ligament, and medial collateral ligament. The femur and tibia were then cut approximately 4 in. from the joint line to obtain an intact joint. From this point forward, the joint was maintained in phosphate buffered saline (PBS) soaked gauze to avoid dehydration.

The femur and tibia were potted in ortho-jet acrylic resin (polymethyl methacrylate, from Lang Dental, Wheeling, IL) using Delrin molds for gripping in an MRI-compatible custom-built loading frame (Fig. 1(*a*)). The embedded tibia is secured via plastic set screws in a cup attached to the bottom of the frame, and the embedded femur is secured in a cup attached to a threaded rod that slides freely through a hole in the top of the frame. The displacement of the rod and hence the femur are fixed in place via lock nuts. For this study, the tibia cup was angled to produce 30 deg joint flexion to match previous studies because this is approximately the maximum extension in the pig, representing 0 deg flexion in a standing human [22,31]. Fluoroscopy was used to adjust and confirm joint alignment, including parallel alignment of the tibia and femur within the molds.

The intact case was an intact joint, where the joint capsule and lateral and medial collateral ligaments were preserved and the musculature removed, prepared as described above. In the tear case, a medial meniscus root tear was created by transection of the anterior attachment (destabilization of the medial meniscus, DMM, a frequently used animal model of OA) using a minimally invasive anterior approach to limit the size of the incision in the joint capsule [3,4,27,28]. The attachment was severed via a horizontal cut along the bone insertion. The attachments are shown by the arrows in Fig. 1(*b*), and the cut was made inferior to this imaging plane along the bone. The repair was done by an experienced veterinary surgeon (TPS) using a SwivelLock suture anchor (Arthrex) placed into the bone such that the meniscus was restored to its original intact position via sutures running from the anchor through the anterior attachment. This is a technique used for root tear surgical repair in humans [32–34].

Joint Loading and Magnetic Resonance Images. To non-invasively measure joint kinematics, MRI were acquired at two loading states. For this experiment, we used a preload (low load) of 44.5 N (10 lbf) and a high load of 850 N or approximately 1.5× body

[2]sierra-medical.com

weight (15-month-old male Yucatan weighs ~60 kg). The low load ensured the joint was in contact, and the high load ensured a physiologic loading to produce joint displacements. Low load was applied by placing a mass on the upper nut on the threaded rod, then immediately locking in the displacement using the bottom nut. For high load, the joint was loaded using a mechanical test instrument (TA Electro-Force 3510, TA Instruments, New Castle, DE) pressing on the threaded rod. Load was applied by manually moving the crosshead at ~0.05 mm/s until the target 850 N load was reached, holding displacement for 10 s to check the loading device alignment, and reapplying the target load. At this point, the nuts on the threaded rod were immediately tightened until zero loads were read by the test instrument's load cell. This resulted in complete load transfer to the loading frame and locked in the applied displacement, preventing further tissue deformation, although stress relaxation continued to occur. MRI was consistently acquired 30 min after the displacement was locked to allow time to transfer from the mechanical tester to the MRI center.

MRI was performed on each joint after low load and high load using the same protocol. Two four-channel surface coils were wrapped around the joint using Velcro, and a T_1 vibe sequence was run to image the joint at high resolution (repetition time = 10 ms, echo time = 3.45 ms, voxel size = 0.2 mm × 0.2 mm × 0.2 mm, runtime = 18 min, Figs. 1(*b*) and 1(*c*)). This sequence was adapted from bone MRI [35,36], and new parameters used here were developed in pilot studies by optimizing the sequence for meniscus signal intensity. After high load imaging, residual (relaxed) load was measured by remounting the loading frame in the TA Electro-Force 3510 (New Castle, DE) and releasing the lock nuts.

Each joint was loaded and imaged in three different experimental states: intact, tear, and repair. After initial loading and MRI in the intact state, joints were wrapped in PBS-soaked gauze and refrigerated at 4 °C overnight to equilibrate under zero applied load. The next day, the tear case was created via release of the anterior attachment 30 min before loading, and loading and MRI were repeated using the same protocol as above. Joints were frozen after tear MRI so that repairs could be done as a batch. Loading and MRI protocols were repeated on the repaired joints either on the same day as the repair procedure or the following day after overnight refrigeration.

Magnetic Resonance Image Analysis. Displacements of the medial meniscus and femoral condyles in the intact, tear, and repair conditions were measured from the MRI images relative to the intact low load position. First, the intact low load image was resliced into the scanner RAS+ (right, anterior, and superior positive) coordinate system, with 0.2 mm isotropic voxels. Next, a tibia-aligned coordinate system was defined. Then, a partial segmentation of the tibia was made using ITK-SNAP's active contour semi-automatic segmentation tool [37]. The tibia coordinate system and segmentation were created in the intact low load image, and the five other images (intact high load, tear low and high load, and repair low and high load) were aligned to this coordinate system by rigid registration of the tibia, using the segmentation as a registration mask [21,22,38]. All registrations were visually checked to confirm alignment of the tibia across all six conditions. All meniscus and femur displacements were calculated in tibia-aligned coordinates with medial, anterior, and inferior assigned as the positive directions. After coordinating alignment, displacements were measured as described below.

To measure meniscus displacement, the outer edge of the medial meniscus was traced in 3D following a line on the outer surface halfway between the superior and inferior rims. This labeling was done for all conditions in the tibia aligned coordinate system. Displacements were measured from intact low load to each high load condition by matching points at the same % arc length along the traced outer edge lines and subtracting their positions. To measure the change in starting position due to treatment, displacements were also measured in the same way for tear and repair low load relative to intact low load. For regional analysis, the points comprising the outer edge line and their associated displacement values were grouped into equal thirds: the anterior region (AR), medial region (MR), and the posterior region (PR) (Figs. 2(*c*)–2(*e*)).

Displacements of the medial and lateral femoral condyles were measured at the points where the condyles contacted the tibial plateau in the intact low load image. These contact points were labeled using 3D SLICER in the aforementioned tibia-aligned coordinate system [39]. The femur was then automatically segmented, and the segmentation was used as a mask for rigid registration of the femur between the intact low load condition and the other five conditions. The resulting rigid transform matrices were applied to the intact low load positions of the two condylar contact points to calculate their displaced positions. Displacements were then calculated by subtracting the intact low load positions from the positions in each other condition.

A repeated measures analysis of variance was used to test for the effect of treatment (intact, tear, repair) on the meniscus and femoral condyle displacements using JMP 16 (JMP, Cary, NC). If significance was met, a posthoc Tukey-test was carried out to test for differences

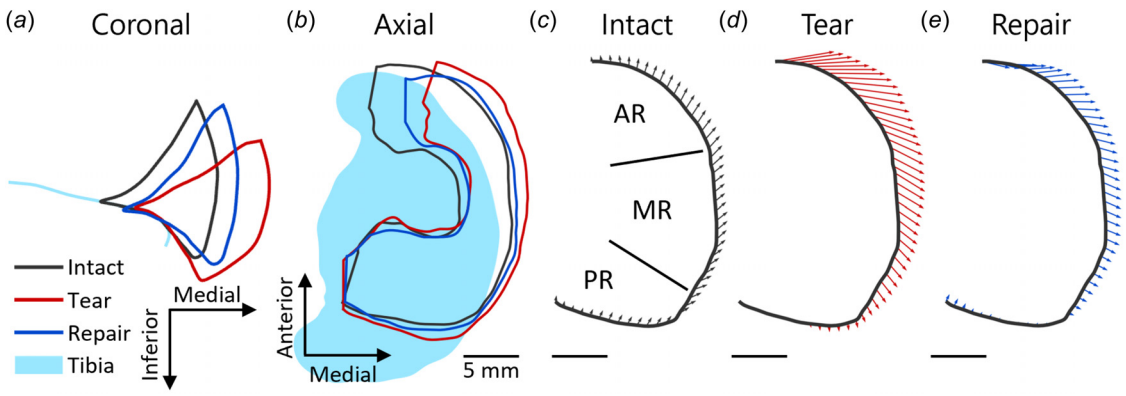

Fig. 2 Representative example of meniscus displacements at high load with each treatment. (*a*) Midcoronal outlines show that the tear allowed the meniscus to be pushed out of the joint space passed the edge of the tibia, while the repair partially restored the meniscus position toward the intact case. (*b*) Axial plane outlines show the same, while also illustrating that the anterior part of the meniscus is displaced more than the posterior. (*c*) Region labels (AR, MR, and PR) for a representative sample of displacements from intact low load to treatment high load for (*c*) intact, (*d*) tear, and (*e*) repair treatment. The anterior region of the meniscus had large medial displacements following tear that were reduced with repair. The MR had moderate displacements that increase with tear and moved posteriorly, while the PR had small displacements.

between treatment groups. Pearson's correlations were performed to test for relationships of the displacements between regions and between the meniscus and femoral condyle. Significance was set at $p < 0.05$. A priori power analysis concluded that $n = 7$ samples were sufficient for a repeated measures design with power = 0.8 and alpha = 0.05 to detect effect sizes of 0.5.

Results

Meniscus Displacements. Qualitatively, the midcoronal outline (Fig. 2(*a*)) and outer boundary (Fig. 2(*b*)) of the meniscus under loading revealed that the meniscus was extruded outside of the joint space passed the edge of the tibia following tear. Repair partially restored the original position of the meniscus within the joint space. In all treatment groups, high load caused the meniscus to partially extrude from the joint space, consistent with uninjured human studies (Figs. 2(*a*) and 2(*b*)) [19,20]. The midcoronal slice was defined in the intact low load case, then the same slice was traced for all other conditions. The largest intact low load → treatment high load displacements occurred in the anterior meniscus, which moved medially out of the joint space passed the edge of the tibia, whereas the posterior meniscus showed little displacement, probably due to the still-intact posterior attachment (Fig. 2(*b*)). Based on this, the meniscus displacements were averaged within three regions of interest: AR, MR, and PR (Fig 2(*c*)). Quantitative analyses supported these observations, as shown by the displacement vectors from intact low load to intact high load (Fig. 2(*c*)), tear high load (Fig. 2(*d*)), and repair high load (Fig. 2(*e*)) for a representative

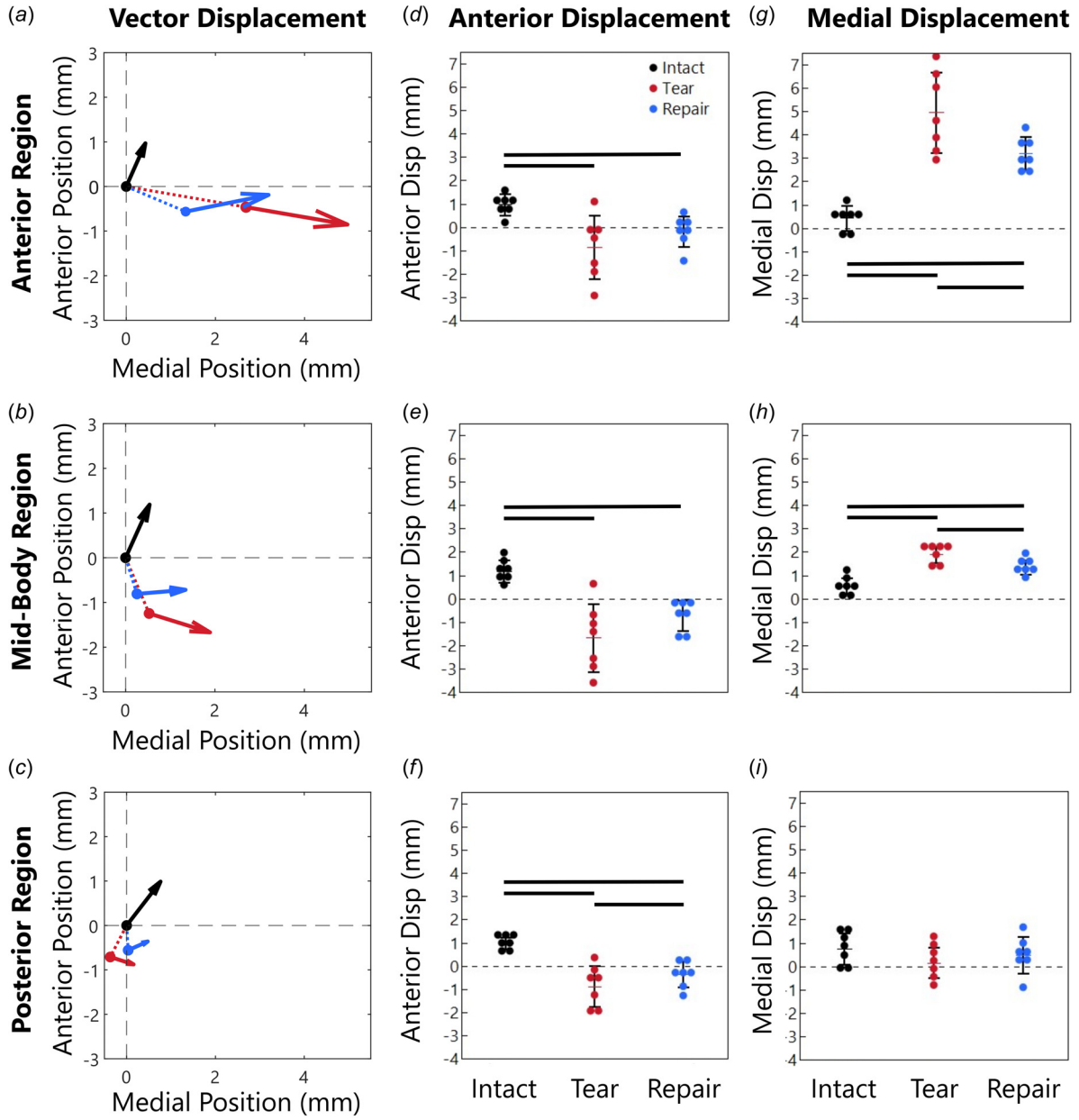

Fig. 3 Meniscus position at high load (arrow head) and low load (arrow origin) averaged in the (*a*) anterior region (AR), (*b*) midbody region (MR), and (*c*) posterior region (PR). Arrowhead size is related to displacement distance. The dashed lines in (*a*–*c*) show displacement from the intact low load position to the tear and repair low load initial positions (additional information provided in Supplemental Materials on the ASME Digital Collection). The total displacement vector for each case, intact low load to intact/tear/repair high load, is decomposed into (*d*–*f*) anterior displacement components and (*g*–*i*) medial displacement components. All meniscus regions displaced posteriorly after the tear (*d*–*f*) and the AR and MR displaced medially (*g*–*i*). The repair generally reduced the large displacements induced by the tear but did not completely restore the intact displacements.

sample. For the AR, at intact high load, displacements were small and mostly uniform (Fig. 2(*c*)). However, following tear and repair there were large medial displacements at this location (Figs. 2(*d*) and 2(*e*)). In addition, small anterior displacements in the intact case changed direction for tear and repair and were on average posterior in both the AR and MR regions. In contrast, the PR had small displacements in all conditions (Figs. 2(*c*) and 2(*e*)).

Average displacement vectors of the outer meniscus boundary in each region were quantified under high load relative to the intact low load (Figs. 3(*a*)–3(*c*), arrowhead size is related to displacement distance.). For statistical analyses, we considered each vector component (anterior and medial directions) (Figs. 3(*d*)–3(*i*)). The AR and MR had significant effects of treatment in both directions ($p < 0.05$), but the PR only had a significant effect of treatment in the anterior direction ($p = 0.02$ for anterior direction and $p = 0.06$ for medial direction), posthoc statistics are described below.

For the intact case, the AR moved 0.97 mm anteriorly and 0.43 mm medially (Figs. 3(*d*) and 3(*g*)). With a tear, the AR moved 0.85 mm predominately posteriorly (similar magnitude but in the opposite direction compared to intact, $p < 0.05$) and 4.96 mm medially out of the joint space (11.5-fold intact, $p < 0.05$, Figs. 3(*d*) and 3(*g*)). With repair, the AR displacements were smaller, moving only 0.19 mm posteriorly ($p < 0.05$) and 3.19 mm medially (7.4-fold intact, $p < 0.05$). While the repair reduced the meniscus displacement, it did not return to intact levels. The vector visualization shows that in the AR the tear caused large medial displacements and small posterior displacements and that the medial displacements were partially restored with repair (Fig. 3(*a*)).

The meniscus displacement changes were similar in the MR compared to the AR, but with lower magnitudes overall (Figs. 3(*e*) and 3(*h*)). For the intact case, the MR displaced 1.19 mm anteriorly and 0.54 mm medially, and with the tear the MR displaced 1.66 mm predominately posteriorly (opposite direction from intact, $p < 0.05$) along with 1.89 mm of medial displacement (3.5-fold intact, $p < 0.05$). With repair, the displacement again decreased compared to tear, but the MR still displaced 0.72 mm predominately posteriorly (opposite of intact, $p < 0.05$) and 1.34 mm medially (2.5-fold intact, $p < 0.05$). The MR moved more posteriorly and less medially than the AR. The vector visualization demonstrates that in the MR, the tear caused large posterior displacements that were partially restored with repair and that the medial displacements were overall smaller than in the AR region (Fig. 3(*b*)).

The PR had the smallest displacement in both directions, with statistical significance between treatments only in the anterior direction ($p = 0.02$ for anterior direction and $p = 0.06$ for medial direction). The intact PR only displaced 0.99 mm anteriorly and 0.76 mm medially (Figs. 3(*f*) and 3(*i*)). With a tear, the PR displaced 0.88 mm posteriorly (opposite direction from intact, $p < 0.05$), but little medially (0.16 mm, 0.2-fold intact). With the repair, the displacements were more similar to intact, with 0.36 mm predominately posteriorly (opposite direction from intact, $p < 0.05$) and 0.48 mm medially (0.6-fold intact). The vector visualization demonstrates that, in the intact case, the PR displacements are similar to the AR and MR, but with both tear and repair, PR displacements were much smaller (Fig. 3(*c*)).

We next evaluated correlations between anterior and medial displacements and between regions. Anterior and medial displacement components were strongly correlated in the AR ($R^2 = 0.85$, $p < 0.05$, Fig. 4(*a*)) and the MR ($R^2 = 0.52$, $p < 0.05$) but not in the PR ($R^2 = 0.11$, $p = 0.15$). With high medial displacements, the meniscus moved posteriorly. In contrast, low medial displacements, as in the intact case, caused anterior meniscus displacements. In terms of comparison between regions, the anterior displacement component was strongly correlated between all regions: AR and MR ($R^2 = 0.88$, $p < 0.05$, Fig. 4(*b*)), AR and PR ($R^2 = 0.75$, $p < 0.05$), MR and PR ($R^2 = 0.90$, $p < 0.05$). For the medial displacement component, there was a significant relationship only between AR and MR ($R^2 = 0.70$, $p < 0.05$, Fig. 4(*c*)), while the AR to PR ($R^2 = 0.08$, $p = 0.22$) and MR to PR ($R^2 = 0.00$, $p = 0.94$) had no relation, likely due to the small displacement magnitudes in the PR.

Femoral Condyle Displacements. In addition to meniscus displacements, we also evaluated the 3D displacements of the medial and lateral femoral condyles at their contact point with the tibial plateau (Fig. 5). For the medial condyle (Fig. 5(*a*)), intact low load → treatment high load displacements were in the anterior, medial, and inferior directions for all treatments. Differences between treatment groups were nonsignificant, but barely so ($p = 0.06$ anterior direction, $p = 0.08$ medial direction, and $p = 0.11$ inferior direction). Anterior displacement of the medial condyle was 2.76 mm for the intact case. This was reduced to 2.03 mm with tear but returned to 2.53 mm with repair, nearly the intact value. Medial displacement in the intact case was 0.42 mm, which was 3.5-fold larger with tear (1.54 mm). With repair, medial displacement was partially restored (1.23 mm), but was still three-fold larger than intact. In the inferior direction, the medial condyle displacement was 1.26 mm for intact. While not significant, in the tear and repair cases, the inferior displacement was slightly larger than intact (1.40 mm and 1.51 mm, respectively). The lateral condyle, similar to the medial condyle, displaced in the anterior, medial, and inferior directions for all treatments, and there were no significant differences with treatment ($p = 0.08$ anterior direction, $p = 0.08$ medial direction, and $p = 0.09$ inferior direction). Lateral condyle displacement results are provided in the Supplemental Materials on the ASME Digital Collection. Overall, despite lack of significance, these results suggest that severing the anterior medial meniscus attachment (tear group) likely altered the displacement of

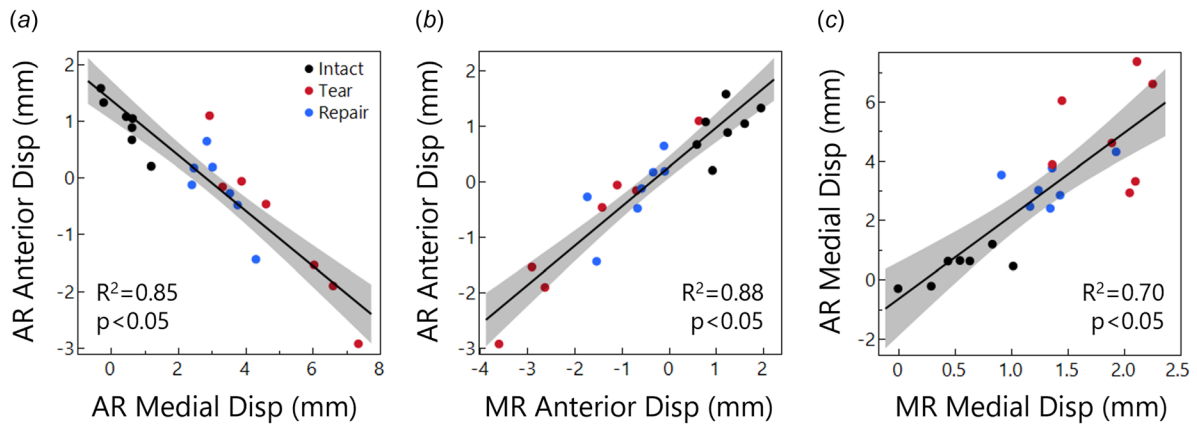

Fig. 4 (*a*) Relationship between AR anterior and medial displacement. Greater medial displacement caused posterior displacement. (*b*) Relationship between AR and MR anterior displacement. (*c*) Relationship between AR and MR medial displacement.

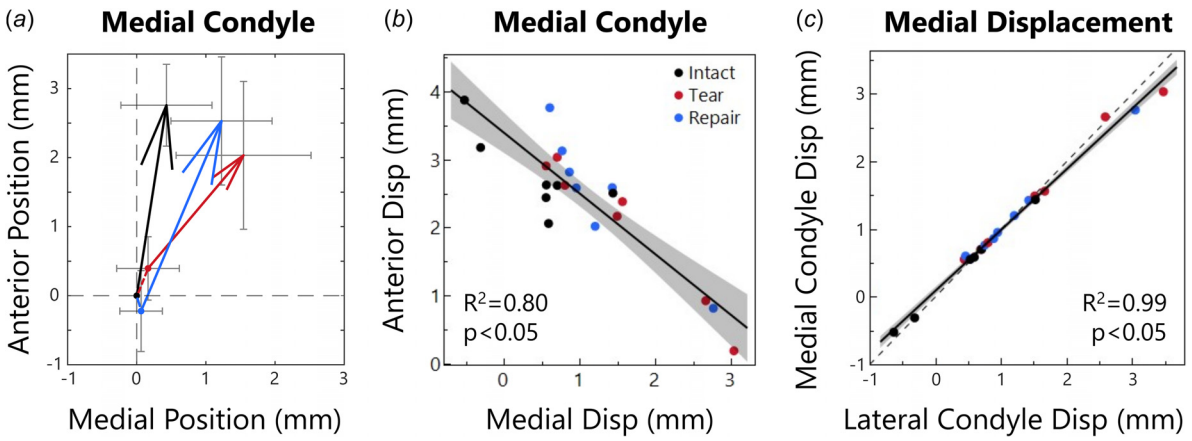

Fig. 5 (*a*) Medial condyle positions at low load (arrow origin) and at high load (arrowhead). Intact joints move anteriorly about 2.76 mm and medially <0.5 mm. The tear case allowed the contact points to shift only 2.03 mm anteriorly but 1.54 mm medially. Repair made motion more similar to intact with 2.53 mm anterior and 1.23 mm medial displacement. Arrowhead size is related to displacement distance. (*b*) Relationship between medial condyle anterior and medial positions. As the condyle moves further medially, it moves less anteriorly. (*c*) Medial versus lateral condyle displacement in the medial direction. The relation is nearly perfectly 1:1 (dashed line).

the femur relative to the tibia, and repair appears to have partially restored the kinematics toward that of the intact condition.

There was a strong correlation between the medial condyle's anterior and medial displacement components ($R^2 = 0.80$, $p < 0.05$, Fig. 5(*b*)), similar to the meniscus. While there was a low correlation between the anterior and inferior displacement ($R^2 = 0.27$, $p < 0.05$), there was a moderate correlation between the medial and inferior displacement ($R^2 = 0.47$, $p < 0.05$), likely related to the slope of the tibial plateau. The lateral condyle exhibited similar correlations between displacement components. As expected for a rigid body, displacements of the medial and lateral condyle were significantly correlated in all directions, including anterior ($R^2 = 0.41$, $p < 0.05$), medial ($R^2 = 0.99$, $p < 0.05$, Fig. 5(*c*)), and inferior ($R^2 = 0.60$, $p < 0.05$).

Correlations Between Meniscus and Femur Displacement. Finally, we evaluated correlations between the meniscus regions and the medial femoral condyle displacements. Considering the meniscus AR, the anterior displacement components of the AR and femoral condyle were correlated ($R^2 = 0.57$, $p < 0.05$, Fig. 6(*a*)). In the tear and repair groups, the meniscus moved posteriorly while the medial condyle moved anteriorly. In the intact case, however, the meniscus moved anteriorly, and the medial condyle moved anteriorly to a greater degree. The medial displacement components of the AR and the medial condyle were also highly correlated ($R^2 = 0.65$, $p < 0.05$, Fig. 6(*b*)). In the tear and repair groups, the meniscus moved much further medially than the condyle (up to 7.4 mm versus up to 3.0 mm, respectively), however, the intact group lies mostly along the 1:1 line where meniscus and condyle motion were equal.

Considering the meniscus MR, the anterior displacement components of the MR and medial condyle were significantly correlated ($R^2 = 0.38$, $p < 0.05$, Fig. 6(*c*)). Menisci in the intact group moved anteriorly, but in the tear and repair groups, the MR moved posteriorly. The medial displacement components of the MR and the femoral condyle were not correlated as strongly as in the AR, but in contrast to the AR region, their relationship followed the 1:1 line very closely, with only slightly more meniscus displacement than contact point displacement ($R^2 = 0.54$, $p < 0.05$, Fig. 6(*d*)). There were no significant relationships between PR meniscus displacement and femoral condyle displacement.

Residual Loads After Imaging. In order to evaluate potential dehydration and effect of load history, we measured residual loads after MRI scanning. Residual loads were 295 N±41N at 68 min±4 min after the load was initially locked into the frame (~65% relaxation from initial load to the end of imaging). These values were not different between treatment groups ($p = 0.68$, analysis of variance, $n = 4$), supporting the use of this loading protocol and sufficient restoration of hydration between repeated loading.

Discussion

In this study, we measured joint kinematics in an intact porcine knee, after anterior root tear, and after repair using noninvasive MRI to maintain an intact joint capsule and surrounding ligaments. We found that transection of the medial meniscus attachment (tear) allows for large amounts of medial extrusion of the medial meniscus, particularly in the anterior region. A suture anchor repair partially restores the meniscus in the joint space and limits femur displacement but does not fully restore kinematics to match the intact case. This study was performed using an MRI-compatible loading device and a newly adapted MRI sequence allowing us to capture the joint structure at multiple loading conditions and with much higher meniscus signal and resolution than previously reported.

We observed meniscus extrusion where the AR had the most displacement while the PR had the least displacement. This can be explained by the posterior attachment behaving like a hinge about which the meniscus pivots. This can be observed in the axial plane for the tear and repair cases where the AR and MR are displaced medially, while the PR remains mostly static due to its posterior attachment (Figs. 2(*b*) and 3). This effect also explains the differences between displacement of the meniscus and of the femur. Though the femur moves anteriorly in all cases due to the 30 deg flexion angle, it moves less anteriorly and more medially after tear and repair, pushing the meniscus AR out of the joint space (Fig. 6). With extrusion, the meniscus pivots about the posterior attachment, and the AR and MR regions of the meniscus move slightly posteriorly. Similar work found that the meniscus of an intact joint instead moved posteriorly with load [22]. The likely cause of this difference in findings is that our study applied load along the femoral axis, pushing the femur forward over the tibia, while [22] applied load along the axial direction of the tibia, pushing the femur backward over the tibia.

Our findings for the femur displacements agree with previous studies of joint kinematics. Studies using pressure sensors placed into the joint space showed that the femoral contact point shifts medially after meniscus injury [2–4,17], similar to our meniscus and femur results. Contact pressure tracking primarily finds that the

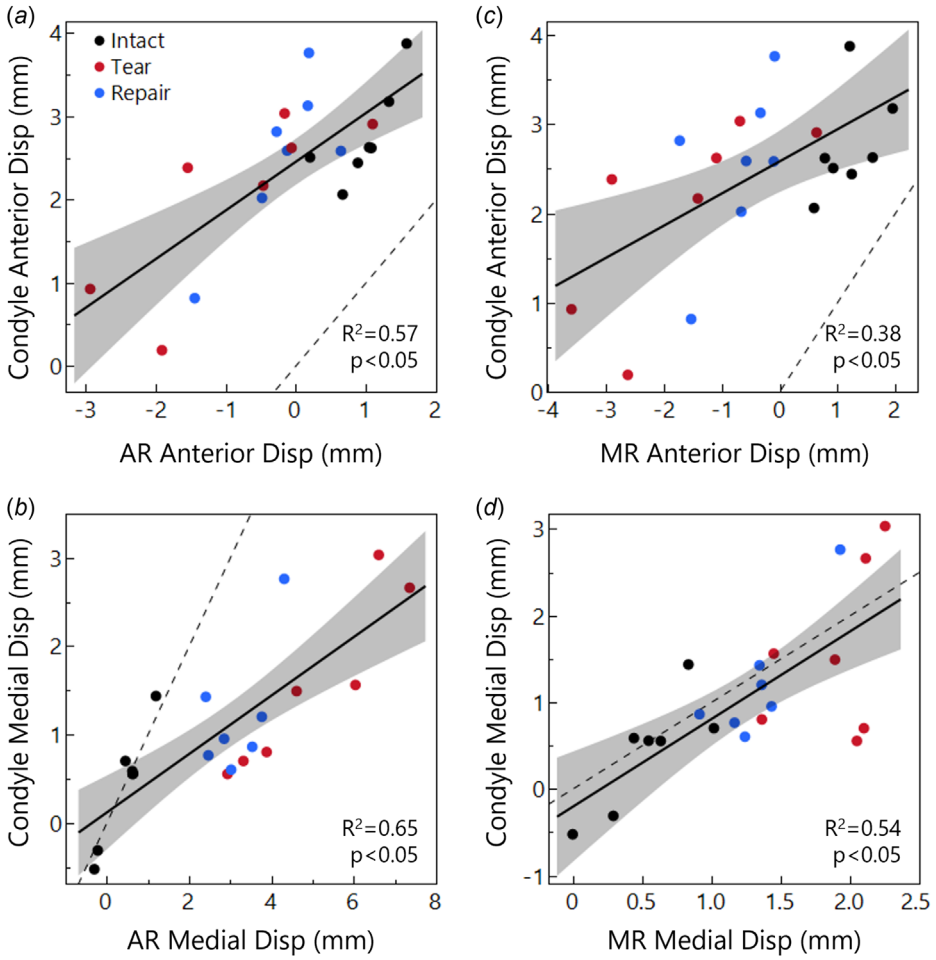

Fig. 6 Displacement relationships between the medial condyle contact point and the meniscus AR (*a* and *b*) and MR (*c* and *d*), considering anterior (*a* and *c*) and medial (*b* and *d*) displacement components. The condyle moves further anteriorly than the meniscus (*a* and *b*), while medial displacements (*b* and *d*) are closer to a 1:1 relationship (dashed line) between the tissues. This 1:1 relationship is lost in the AR with tear and repair conditions because, with the anterior medial meniscus attachment released, the meniscus AR displaces far outside of the joint space with loading.

contact area decreases, indicating that the meniscus is not carrying load due to extrusion by the femur. This matches what we find when we track both the femur and meniscus in our study. After tear, the femur moves medially and anteriorly, pushing the meniscus, especially the anterior region, out of the joint, so that the meniscus is no longer carrying load or distributing forces to protect the cartilage. This is likely linked to the higher rates of OA seen in many patients with high meniscus extrusion or after meniscus root tear [12–14].

The large displacements in the repair case, particularly in the AR, suggest that a better surgical treatment might be required to restore joint kinematics to the intact state. The suture anchor repair returns the anterior aspect of the meniscus back to its natural position by suturing through the cut anterior attachment. Due to the highly aligned fiber structure of the attachment, it is possible that the anchor did not adequately hold the meniscus in place due to the sutures pulling through the weaker interfiber matrix when load was applied. However, this study explored the effectiveness of repair treatment at acute time points, whereas in vivo, there would be time for healing, remodeling, and potentially unloaded postoperative care. Thus, further, in vivo studies are needed to explore if the suture anchor repair aids in healing to increase the strength of the anchor/anterior attachment complex and to reduce medial extrusion of the meniscus under load. Another solution to reduce medial extrusion may be to add sutures on the outside of the joint for meniscus centralization, especially in the anterior half, similar to previous studies [14,17]. Other methods to reduce meniscus extrusion should be explored as well. The methods used in this study are valuable to test other repair strategies to restore joint kinematics and meniscus load distribution to protect the underlying cartilage.

Our novel T_1 vibe MRI sequence for joint imaging allowed for excellent meniscus signal intensity and resolution. Due to the meniscus' densely packed fiber network, MRI signal in most clinical studies and cartilage-focused studies is quite low, such that in most clinical and preclinical research using MRI, the meniscus is a black object between the femur and tibia [40]. With our MRI sequence, we could observe meniscus structure for segmentation and calculation of displacements. T_1 vibe has traditionally been utilized in abdominal, breast, and brain imaging, but has recently been recommended for use in musculoskeletal applications as a replacement for CT due to its ability to provide high resolution bone imaging [35,36]. Before this study, in preliminary work, we optimized the T_1 vibe sequence parameters for meniscus imaging. To our knowledge, we are the first to utilize T_1 vibe in the knee specifically for meniscus motion tracking. Compared to other studies, our images achieve more signal from the meniscus while maintaining higher resolution and/or shorter scan times [12,13,21–23].

This study utilized porcine knees consistent with established animal models for OA in order to provide baseline data for joint

function postinjury and repair in preclinical research. The pig knee is an important model to study meniscus injury and repair in vivo in a way that is not ethically feasible in humans. Because we did not use human knees, the results should not be directly translated to clinical practice, however, the methods used in this paper are applicable to future human study both in vivo and ex vivo. The methods and MRI sequence can be used with human subjects [20,24], however, due to the required scanning in two different loading states, these are more likely to be used in a research setting. Importantly, results utilizing these methods in human subject research will be informative to improve future surgical treatments.

This study is not without limitations. First, though we kept the joint capsule and surrounding ligaments as intact as possible, a small incision was required for creation of the tear and the repair procedure. This was an approximately 3.0 cm vertical incision in the joint capsule to the medial side of the patellar tendon, which is considerably smaller than the incisions or dissections used in other studies using pressure sensors [2–4,17,18]. Second, due to the aligned nature of the meniscus attachment, there is the possibility of suture slippage or pull-out in the repair group. Despite this possibility, after testing, the repair was inspected to confirm that the meniscus was still anchored to the bone as intended. Due to the time required to prepare the samples, the repeated loading with stress relaxation, and the time between loading sessions, it is possible that some dehydration and/or autolysis occurred. We minimized these effects by wrapping the joint in PBS-soaked gauze and refrigerating the unloaded joint at 4 °C between the intact and tear cases. The residual loads did not differ between treatment groups, indicating minimal effect of dehydration and autolysis after repeated loading.

In conclusion, this study found that anterior root tears resulted in large meniscus displacements with loading and that suture anchor repair reduced these displacements but did not restore intact joint kinematics. The femur moved anteriorly in all cases, but further medially after tear and repair. Under load, the anterior region of the meniscus moved posteriorly and medially as it was forced out of the joint space, while the posterior region had small displacements due to the restraint of the posterior attachment, which acted as a hinge about which the meniscus pivoted in the axial plane. The experimental techniques used here can be applied to evaluate the effect of knee injuries and to develop improved repair strategies to restore joint kinematics after injury.

Acknowledgment

We like to thank our funding sources for their contributions to this work.

Funding Data

- National Institute of Arthritis and Musculoskeletal and Skin Diseases (Grant No. 5R01AR050052; Funder ID: 10.13039/100000069).
- National Institute of General Medical Sciences (Grant No. 2P20GM139760; Funder ID: 10.13039/100000057).

Conflict of Interest

We have no conflicts of interest to disclose.

Data Availability Statement

The datasets generated and supporting the findings of this article are obtainable from the corresponding author upon reasonable request.

Author Contributions

KDM, JMP, MIM, and TPS contributed to experiments for the study. KDM, JMP, and MIM contributed to analysis of the study. KDM, JMP, MIM, and DME contributed to results interpretation. All authors contributed to study design and writing the paper and have read and approved submission.

References

[1] Berthiaume, M. J., Raynauld, J. P., Martel-Pelletier, J., Labonté, F., Beaudoin, G., Bloch, D. A., Choquette, D., et al., 2005, "Meniscal Tear and Extrusion Are Strongly Associated With Progression of Symptomatic Knee Osteoarthritis as Assessed by Quantitative Magnetic Resonance Imaging," Ann. Rheum. Dis., **64**(4), pp. 556–563.

[2] Bedi, A., Kelly, N. H., Baad, M., Fox, A. J. S., Brophy, R. H., Warren, R. F., and Maher, S. A., 2010, "Dynamic Contact Mechanics of the Medial Meniscus as a Function of Radial Tear, Repair, and Partial Meniscectomy," J. Bone Jt. Surg. Ser. A, **92**(6), pp. 1398–1408.

[3] Bansal, S., Miller, L. M., Patel, J. M., Meadows, K. D., Eby, M. R., Saleh, K. S., Martin, A. R., et al., 2020, "Transection of the Medial Meniscus Anterior Horn Results in Cartilage Degeneration and Meniscus Remodeling in a Large Animal Model," J. Orthop. Res., **38**(12), pp. 2696–2708.

[4] Bansal, S., Meadows, K. D., Miller, L. M., Saleh, K. S., Patel, J. M., Stoeckl, B. D., Lemmon, E. A., Hast, M. H., et al., 2021, "Six-Month Outcomes of Clinically Relevant Meniscal Injury in a Large-Animal Model," Orthop. J. Sports Med., **9**(11), pp. 1–17.

[5] Lohmander, L. S., Englund, P. M., Dahl, L. L., and Roos, E. M., 2007, "The Long-Term Consequence of Anterior Cruciate Ligament and Meniscus Injuries: Osteoarthritis," Am. J. Sports Med., **35**(10), pp. 1756–1769.

[6] Papalia, R., del Buono, A., Osti, L., Denaro, V., and Maffulli, N., 2011, "Meniscectomy as a Risk Factor for Knee Osteoarthritis: A Systematic Review," Br. Med. Bull., **99**(1), pp. 89–106.

[7] Roos, H., Adalberth, T., Dahlberg, L., and Lohmander, L. S., 1995, "Osteoarthritis of the Knee After Injury to the Anterior Cruciate Ligament or Meniscus: The Influence of Time and Age," Osteoarthritis Cartilage, **3**(4), pp. 261–267.

[8] Hunter, D. J., Zhang, Y. Q., Niu, J. B., Tu, X., Amin, S., Clancy, M., Guermazi, A., Grigorian, M., Gale, D., and Felson, D. T., 2006, "The Association of Meniscal Pathologic Changes With Cartilage Loss in Symptomatic Knee Osteoarthritis," Arthritis Rheum., **54**(3), pp. 795–801.

[9] Biswal, S., Hastie, T., Andriacchi, T. P., Bergman, G. A., Dillingham, M. F., and Lang, P., 2002, "Risk Factors for Progressive Cartilage Loss in the Knee: A Longitudinal Magnetic Resonance Imaging Study in Forty-Three Patients," Arthritis Rheum., **46**(11), pp. 2884–2892.

[10] Persson, F., Turkiewicz, A., Bergkvist, D., Neuman, P., and Englund, M., 2018, "The Risk of Symptomatic Knee Osteoarthritis After Arthroscopic Meniscus Repair vs Partial Meniscectomy Vs the General Population," Osteoarthritis Cartilage, **26**(2), pp. 195–201.

[11] Rockborn, P., and Messner, K., 2000, "Long-Term Results of Meniscus Repair and Meniscectomy: A 13-Year Functional and Radiographic Follow-Up Study," Knee Surg., Sports Traumatol., Arthroscopy, **8**(1), pp. 2–9.

[12] Debieux, P., Jimenez, A. E., Novaretti, J. V., Kaleka, C. C., Kriscenski, D. E., Astur, D. C., Obopilwe, E., Tamburini, L. M., Muench, L. N., Cote, M. P., Cohen, M., and Coyner, K. J., 2021, "Medial Meniscal Extrusion Greater Than 4 mm Reduces Medial Tibiofemoral Compartment Contact Area: A Biomechanical Analysis of Tibiofemoral Contact Area and Pressures With Varying Amounts of Meniscal Extrusion," Knee Surg., Sports Traumatol., Arthroscopy, **29**(9), pp. 3124–3132.

[13] Lerer, D. B., Umans, H. R., Hu, M. X., and Jones, M. H., 2004, "The Role of Meniscal Root Pathology and Radial Meniscal Tear in Medial Meniscal Extrusion," Skeletal Radiol., **33**(10), pp. 569–574.

[14] Ozeki, N., Muneta, T., Kawabata, K., Koga, H., Nakagawa, Y., Saito, R., Udo, M., et al., 2017, "Centralization of Extruded Medial Meniscus Delays Cartilage Degeneration in Rats," J. Orthop. Sci., **22**(3), pp. 542–548.

[15] Sukopp, M., Schall, F., Hacker, S. P., Ignatius, A., Dürselen, L., and Seitz, A. M., 2021, "Influence of Menisci on Tibiofemoral Contact Mechanics in Human Knees: A Systematic Review," Front. Bioengin. Biotechnol., **9**, pp. 1–15.

[16] Gajjar, S. M., Solanki, K. P., Shanmugasundaram, S., and Kambhampati, S. B. S., 2021, "Meniscal Extrusion: A Narrative Review," Orthop. J. Sports Med., **9**(11), pp. 1–10.

[17] Kohno, Y., Koga, H., Ozeki, N., Matsuda, J., Mizuno, M., Katano, H., and Sekiya, I., 2022, "Biomechanical Analysis of a Centralization Procedure for Extruded Lateral Meniscus After Meniscectomy in Porcine Knee Joints," J. Orthop. Res., **40**(5), pp. 1097–1103.

[18] Ozeki, N., Koga, H., Matsuda, J., Kohno, Y., Mizuno, M., Katano, H., Tsuji, K., Saito, T., Muneta, T., and Sekiya, I., 2020, "Biomechanical Analysis of the Centralization Procedure for Extruded Lateral Menisci With Posterior Root Deficiency in a Porcine Model," J. Orthop. Sci., **25**(1), pp. 161–166.

[19] Boxheimer, L., Lutz, A. M., Treiber, K., Goepfert, K., Crook, D. W., Marincek, B., and Weishaupt, D., 2004, "MR Imaging of the Knee: Position Related Changes of the Menisci in Asymptomatic Volunteers," Invest. Radiol., **39**(5), pp. 254–263.

[20] Stehling, C., Souza, R. B., Le Graverand, M. P. H., Wyman, B. T., Li, X., Majumdar, S., and Link, T. M., 2012, "Loading of the Knee During 3.0 T MRI is Associated With Significantly Increased Medial Meniscus Extrusion in Mild and Moderate Osteoarthritis," Eur. J. Radiol., **81**(8), pp. 1839–1845.

[21] Schwer, J., Rahman, M. M., Stumpf, K., Rasche, V., Ignatius, A., Dürselen, L., and Seitz, A. M., 2020, "Degeneration Affects Three-Dimensional Strains in Human Menisci: In Situ MRI Acquisition Combined With Image Registration," Front. Bioeng. Biotechnol., **8**, pp. 1–12.

[22] Freutel, M., Seitz, A. M., Galbusera, F., Bornstedt, A., Rasche, V., Knothe Tate, M. L., Ignatius, A., and Dürselen, L., 2014, "Medial Meniscal Displacement and Strain in Three Dimensions Under Compressive Loads: MR Assessment," J. Magn. Reson. Imaging, **40**(5), pp. 1181–1188.
[23] Yao, J., Snibbe, J., Maloney, M., and Lerner, A. L., 2006, "Stresses and Strains in the Medial Meniscus of an ACL Deficient Knee Under Anterior Loading: A Finite Element Analysis With Image-Based Experimental Validation," ASME J. Biomech. Eng., **128**(1), pp. 135–141.
[24] Wang, H., Koff, M. F., Potter, H. G., Warren, R. F., Rodeo, S. A., and Maher, S. A., 2015, "An MRI-Compatible Loading Device to Assess Knee Joint Cartilage Deformation: Effect of Preloading and Inter-Test Repeatability," J. Biomech., **48**(12), pp. 2934–2940.
[25] Paranjape, C. S., Cutcliffe, H. C., Grambow, S. C., Utturkar, G. M., Collins, A. T., Garrett, W. E., Spritzer, C. E., and DeFrate, L. E., 2019, "A New Stress Test for Knee Joint Cartilage," Sci. Rep., **9**(1), pp. 1–8.
[26] Sutter, E. G., Widmyer, M. R., Utturkar, G. M., Spritzer, C. E., Garrett, W. E., and Defrate, L. E., 2015, "In Vivo Measurement of Localized Tibiofemoral Cartilage Strains in Response to Dynamic Activity," Am. J. Sports Med., **43**(2), pp. 370–376.
[27] Waller, K. A., Chin, K. E., Jay, G. D., Zhang, L. X., Teeple, E., McAllister, S., Badger, G. J., Schmidt, T. A., and Fleming, B. C., 2017, "Intra-Articular Recombinant Human Proteoglycan 4 Mitigates Cartilage Damage After Destabilization of the Medial Meniscus in the Yucatan Minipig," Am. J. Sports Med., **45**(7), pp. 1512–1521.
[28] Bansal, S., Keah, N. M., Neuwirth, A. L., O'Reilly, O., Qu, F., Seiber, B., Mandalapu, S., Mauck, R. L., and Zgonis, M., 2017, "Large Animal Models of Meniscus Repair and Regeneration: A Systematic Review of the State of the Field," Tissue Eng. Part C Methods, **23**(11), pp. 661–672.
[29] Cope, P. J., Ourradi, K., Li, Y., and Sharif, M., 2019, "Models of Osteoarthritis: The Good, the Bad and the Promising," Osteoarthritis Cartilage, **27**(2), pp. 230–239.
[30] Teeple, E., Jay, G. D., Elsaid, K. A., and Fleming, B. C., 2013, "Animal Models of Osteoarthritis: Challenges of Model Selection and Analysis," AAPS J., **15**(2), pp. 438–446.
[31] Stärke, C., Kopf, S., Gröbel, K. H., and Becker, R., 2009, "Tensile Forces at the Porcine Anterior Meniscal Horn Attachment," J. Orthop. Res., **27**(12), pp. 1619–1624.
[32] Jung, Y. H., Choi, N. H., Oh, J. S., and Victoroff, B. N., 2012, "All-Inside Repair for a Root Tear of the Medial Meniscus Using a Suture Anchor," Am. J. Sports Med., **40**(6), pp. 1406–1411.
[33] Choi, N. H., Son, K. M., and Victoroff, B. N., 2008, "Arthroscopic All-Inside Repair for a Tear of Posterior Root of the Medial Meniscus: A Technical Note," Knee Surg., Sports Traumatol. Arthroscopy, **16**(9), pp. 891–893.
[34] Kim, J. H., Shin, D. E., Dan, J. M., Nam, K. S., Ahn, T. K., and Lee, D. H., 2009, "Arthroscopic Suture Anchor Repair of Posterior Root Attachment Injury in Medial Meniscus: Technical Note," Arch. Orthop. Trauma Surg., **129**(8), pp. 1085–1088.
[35] Katakura, M., Mitchell, A. W. M., Lee, J. C., and Calder, J. D., 2020, "Is It Time to Replace CT With T1-Vibe MRI for the Assessment of Musculoskeletal Injuries?," Bone Jt. J, **102-B**(11), pp. 1435–1437.
[36] Koh, E., Walton, E. R., and Watson, P., 2018, "VIBE MRI: An Alternative to CT in the Imaging of Sports-Related Osseous Pathology?," Br. J. Radiol., p. 20170815.
[37] Yushkevich, P. A., Piven, J., Hazlett, H. C., Smith, R. G., Ho, S., Gee, J. C., and Gerig, G., 2006, "User-Guided 3D Active Contour Segmentation of Anatomical Structures: Significantly Improved Efficiency and Reliability," Neuroimage, **31**(3), pp. 1116–1128.
[38] Arno, S., Chaudhary, M., Walker, P. S., Forman, R., Glassner, P., Regatte, R., and Oh, C., 2012, "Anterior-Posterior Stability of the Knee by an MR Image Subtraction Method," Knee, **19**(4), pp. 445–449.
[39] Fedorov, A., Beichel, R., Kalpathy-Cramer, J., Finet, J., Fillion-Robin, J. C., Pujol, S., Bauer, C., Jennings, D., Fennessy, F., Sonka, M., Buatti, J., Aylward, S., Miller, J. V., Pieper, S., and Kikinis, R., 2012, "3D Slicer as an Image Computing Platform for the Quantitative Imaging Network," Magn. Reson. Imaging, **30**(9), pp. 1323–1341.
[40] Nacey, N. C., Geeslin, M. G., Miller, G. W., and Pierce, J. L., May 2017, "Magnetic Resonance Imaging of the Knee: An Overview and Update of Conventional and State of the Art Imaging," J. Magn. Reson. Imaging, **45**(5), pp. 1257–1275.